

INFLUENCES OF PROCESS PARAMETERS ON THE QUALITY OF HYDROXYAPATITE COATING ON AZ91 MAGNESIUM ALLOY

Sevda ALBAYRAK¹, Henifi ÇİNİCİ¹, Recep ÇALIN², Canser CÖMERT¹

¹Gazi University, Department of Metallurgical and Materials Engineering, Ankara-TURKEY

²Kırıkkale University, Department of Metallurgical and Materials Engineering, Kırıkkale-TURKEY

¹sevdatas@gazi.edu.tr, ¹hcinici@gazi.edu.tr
²recepcalin@hotmail.com, ¹comertcanser@gmail.com

Abstract: Biodegradable materials such as AZ91 magnesium alloy arouse most of the researchers' interest in recent years. AZ91 Magnesium alloy is a potential alloy in order to use in biomaterial applications as it is both light and similar to the mechanical features of bone. However, this alloy shows corrosive behavior (in biological environment) in human body. Extensive studies have been conducted to use of AZ91 Mg alloy as a biodegradable material. This study focuses on the use of AZ91 Mg alloy as a permanent implant. As it is necessary to prevent the corrosion of such alloy in the body, its surface was coated by sol-gel method with hydroxyapatite material which has sufficient strength and tissue compatibility. The effects of process parameters, i.e. different dipping numbers of sol-gel coating at the coating stage and different sintering temperatures of these coatings, on coating quality was analyzed with Scanning Electron Microscopy (SEM) and x-ray diffractometer (XRD).

Keywords: AZ91 magnesium alloy, hydroxyapatite, Sol-gel coating method

Introduction

AZ91 Magnesium alloy is a potential alloy in order to use in biomedical applications as it is both lightweight and similar to the mechanical features of human bone particularly it shows similar Young's modulus to bone. Lightness is extremely important in biomedical applications because stainless steel and many of the similar metallic alloys can lead to infection by causing harm to tissues around the implant when it is used in the body (Wang, M.J., Chao, S.C., & Yen, S.K., 2016; Surmeneva, M.A. & Surmenev, R.A. , Microstructure characterization and corrosion behaviour of a nanohydroxyapatite coating deposited on AZ31 magnesium alloy using radio frequency magnetron sputtering, 2015; Liu, G.Y. , Hu, J. , Ding, Z.K. , & Wang, C. , Formation mechanism of calcium phosphate coating on micro-arc oxidized magnesium, 2011; Liu, G.Y. , Hu, J. , Ding, Z.K., & Wang, C. , Bioactive calcium phosphate coating formed on micro-arc oxidized magnesium by chemical deposition, 2011; Niu, B., ve diğerleri, 2016). However, its biodegradable behavior in biological environment restricts its use (Surmeneva, M.A., ve diğerleri, 2015; Niu, B., ve diğerleri, 2016). Various studies have been conducted to reduce its degradation rate; process modification, alloying of the magnesium and surface coating techniques (Chen, X.-B. , Birbilis, N. , & Abbott, T.B. , 2012; Hiromoto, S. & Tomozawa, M., Hydroxyapatite coating of AZ31 magnesium alloy by a solution treatment and its corrosion behavior in NaCl solution, 2011; Xu, L., ve diğerleri, 2009) for instance electrophoretic deposition, electrochemical deposition, sol-gel and dip coating have been widely studied. Corrosion preventive coatings for AZ91 magnesium alloy is very important to develop its usage area (Hiromoto, S. & Yamamotoa, A., High corrosion resistance of magnesium coated with hydroxyapatite directly synthesized in an aqueous solution, 2009).

Hydroxyapatite is a bioceramic material widely used in medicine and dentistry and a calcium phosphate-based material forming the inorganic structure of bone tissue (Kannan, M. B., 2015). HAp has almost the same chemical composition and structure as human bone (Rojace, R., Fathi, M., & Raeissi, K., 2014). Because of its biocompatibility, it is used in the construction of various prosthesis, repairing of cracks and broken bones and coating of metallic biomaterials as an artificial bone (Hiromoto, S. & Tomozawa, M., Hydroxyapatite coating of AZ31 magnesium alloy by a solution treatment and its corrosion behavior in NaCl solution, 2011).

In this study, AZ91 Mg alloy was produced with hot press sintering method and coated with hydroxyapatite using combination of sol-gel and dip coating method. The effects of sintering temperature and dipping number on the quality of surface coating was investigated. Surface morphology and phase structure evaluation of the coatings were analyzed with SEM and XRD, respectively.

Materials and Methods

Sample Preparation

AZ91 magnesium alloy powders were sintered at a pressure of 275 MPa at 325 °C for a period of 1 h with unidirectional hot pressing. Produced AZ91 Mg alloy was cut in to 60×10×8 mm pieces. The specimens were mechanically ground with SiC papers and finished with 1200 grit, then polished with 6 and 3 μ diamond suspension. Cleaning process was followed by dipping the specimens in acetone and ethanol in ultrasonic bath for 10 and 20 minutes, respectively.

Calcium nitrate tetra hydrate (Ca(NO₃)₂·4H₂O) and phosphorous pentoxide (P₂O₅) were selected as Ca and P precursors and dissolved separately in ethanol. Ca precursor was added drop wise to P precursor and then stirred at ambient temperature for 5 hours.

The specimens were dipped the number of 1, 3, and 5 vertically into the prepared solution and pulled off at the speed of 6 mm/min by an electrical dip coater. The dip coated specimens were maintained at room temperature for 24 hours to complete the aging process. Then, they were dried at 60 °C for 24 hours and sintered to 300 °C, 400 °C, and 500 °C for 6 hours (heating rate: 5 °/min.). The codes of the specimens are given in **Table 1**.

Table 1: Code-designated specimens.

Number of dipping →	1 dip	3 dip	5 dip
Sintering temperature ↓			
300 °C	1-300	3-300	5-300
400 °C	1-400	3-400	5-400
500 °C	1-500	3-500	5-500

Characterization

The surface and the cross-section morphologies of the specimens were obtained by a scanning electron microscope (SEM). The phases of the coatings sintered at different temperatures and different number of dipping were determined by X-ray diffraction (XRD) technique with a CuKα wavelength of 1.5418 (Å). The settings of diffractometer were adjusted to 40 kV and 30 mA at a 2θ range of 25-70 ° employing a step size of 0.02 °/s.

Results and Discussion

The surface of morphologies of the specimens prepared under different sintering temperatures and dipping numbers are shown in **Fig. 1**. It is obviously seen that coatings fully cover the substrate but there are a lot of cracks on the surface. Crack formation could be resulted from the stresses when volatile constituents escape from the material surface at the sintering stage. And the amount of the cracks and crack area portion decrease with increasing dip number.

The cross-section micrographs of the specimens are shown in **Fig. 2**, which reveals coating thickness of about 3 μm. The coating thickness of the specimens increase with increasing dip number and decrease with increasing sintering temperature.

The distribution of elements in the coatings is given by the EDS analysis in **Table 2**, which indicates the presence of O, Mg, Al, P and Ca. According to the EDS results coating layer consists substrate major element and at the same time the substrate consists the coating elements, too. So, although there are a lot of cracks on the surfaces, the coating layer and substrate are integrated each other.

Fig. 3, Fig. 4, and Fig. 5 shows the XRD patterns of the coatings sintered at stable temperature with 1, 3 and 5 dip numbers and pure AZ91 Mg alloy; **Fig. 6, Fig. 7, and Fig. 8** shows the XRD patterns of the coatings sintered at 300, 400, and 500 °C with stable dip number and pure AZ91 Mg alloy. α, β, and γ represent Mg, Mg₁₇Al₁₂, and hydroxyapatite phases, respectively. Phases were determined according to the literature (Hou, Liang, Chen, Dong, & Han, 2015; Razavi, ve diğerleri, 2014; Kabirian & Mahmudi, 2009; Lee, Pai, & Chang, 2013). AZ91 Mg alloy used in present study was composed of Mg phase together with some Mg₁₇Al₁₂ phase as stated in the literature. Coating and substrate peaks cannot be distinguished from each other. This may be due to the average up to 3 micrometers thin film coating layer. As the number of dip and sintering temperature increased, the new γ peaks are formed and the intensity of AZ91 peaks are decreased.

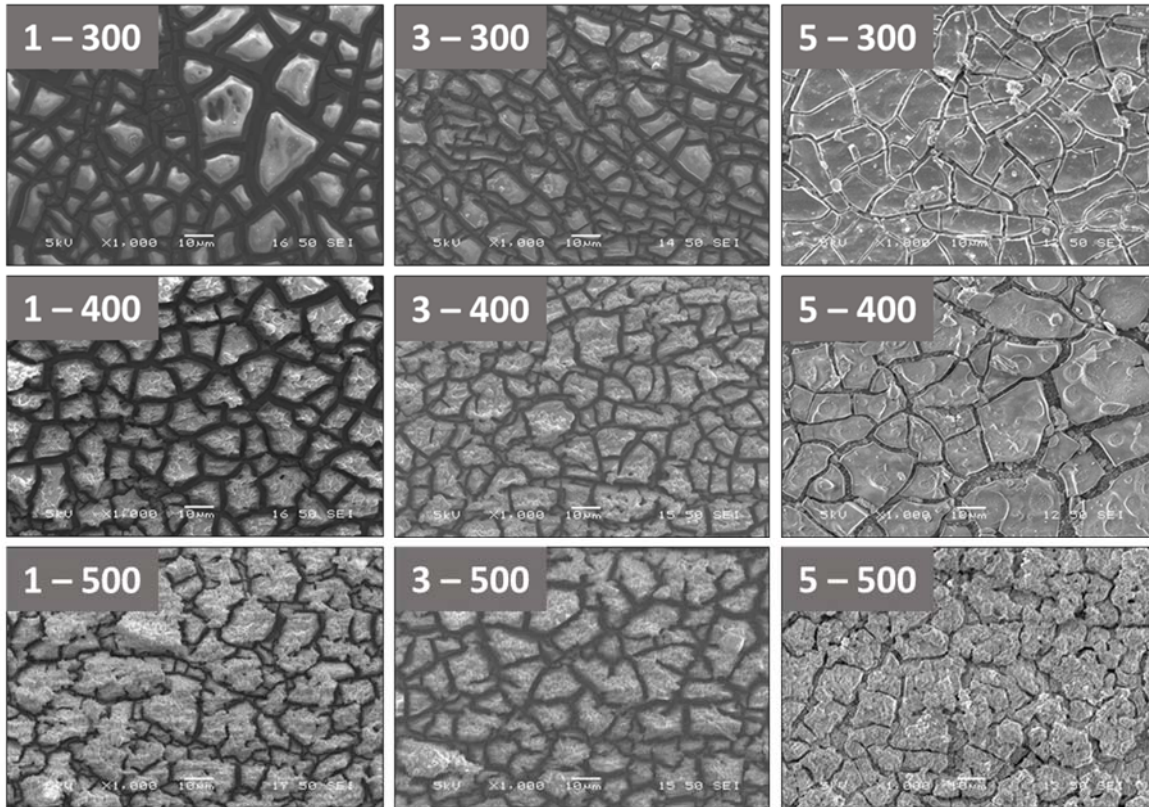


Figure 1. SEM images of the specimens at a magnification of 100x.

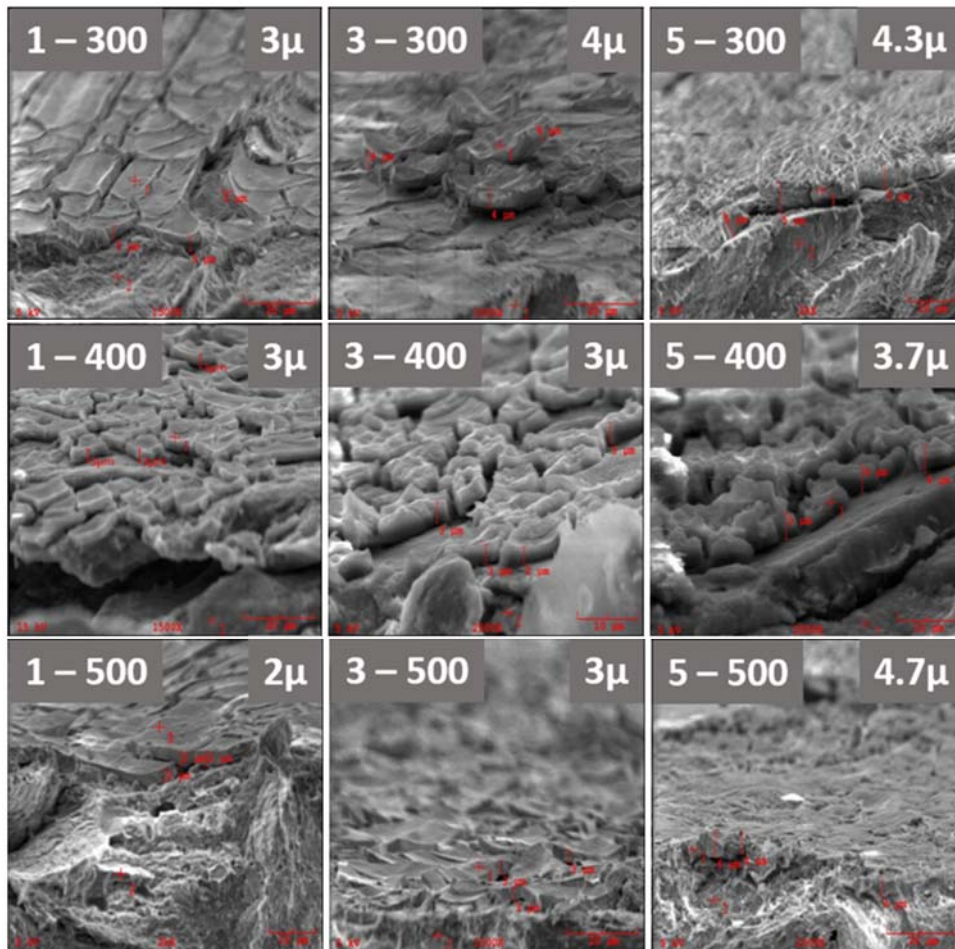


Figure 2. Cross section and EDS analysis of the specimens.

Table 2: The average value of point EDS analysis of specimens given in Fig. 2.

Element	O		Mg		Al		P		Ca	
Point	1	2	1	2	1	2	1	2	1	2
Average	8.434	3.227	12.071	76.473	1.747	2.528	11.375	2.160	66.373	15.612

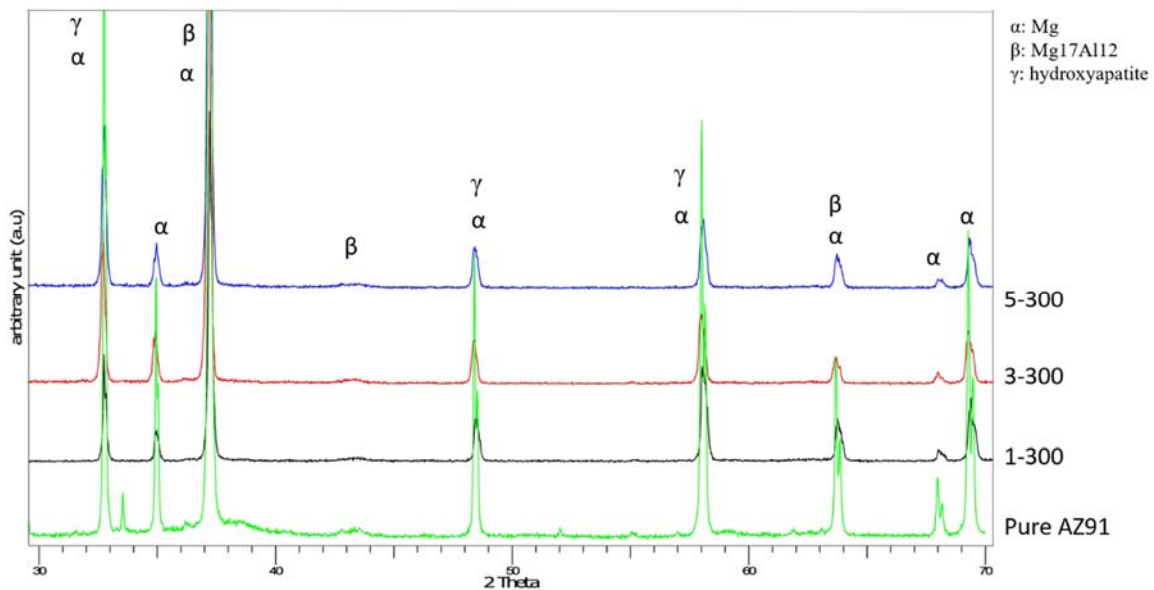


Figure 3. XRD patterns of the coatings sintered at 300 °C with 1, 3 and 5 dip numbers and pure AZ91 Mg alloy.

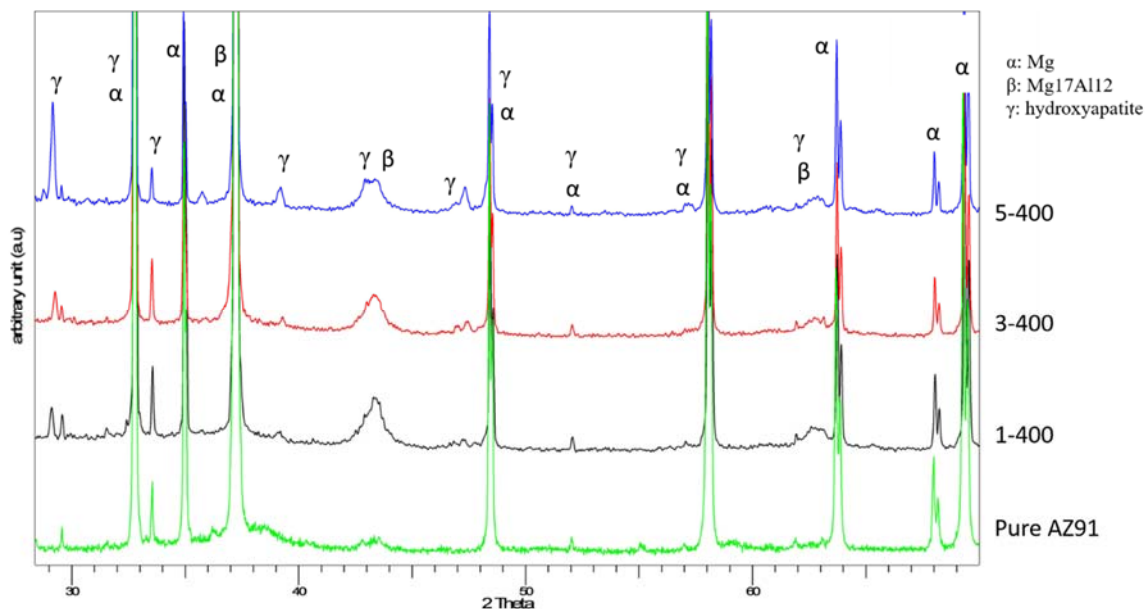


Figure 4. XRD patterns of the coatings sintered at 400 °C with 1, 3 and 5 dip numbers and pure AZ91 Mg alloy.

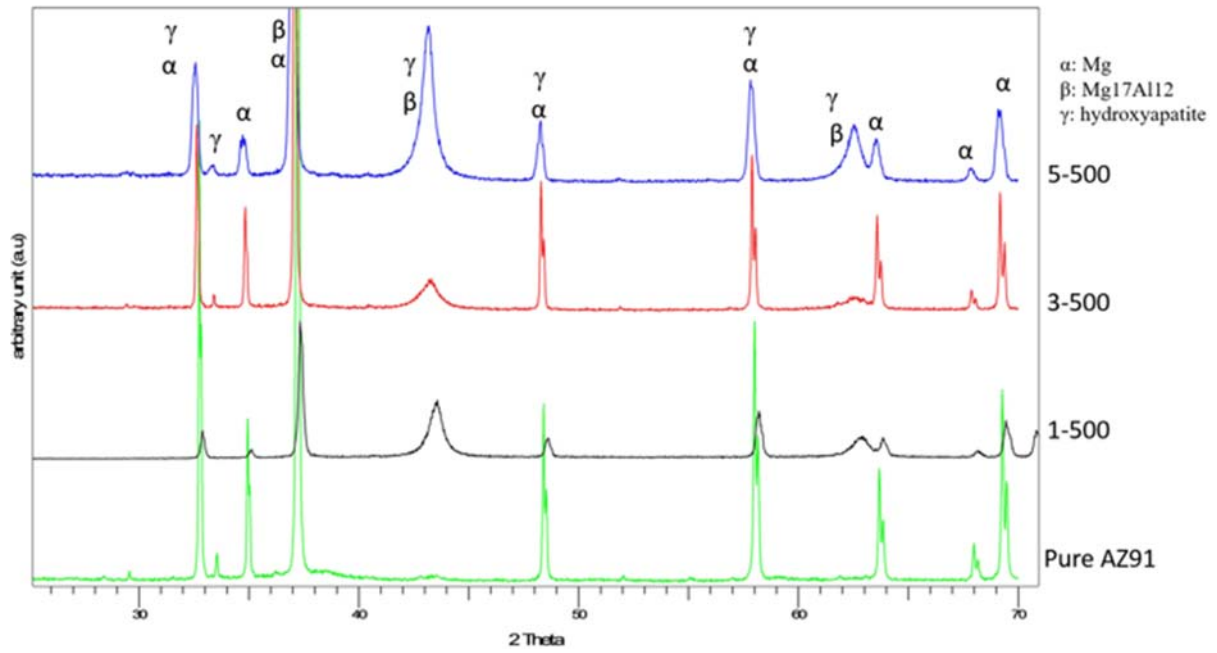


Figure 5. XRD patterns of the coatings sintered at 500 °C with 1, 3 and 5 dip numbers and pure AZ91 Mg alloy.

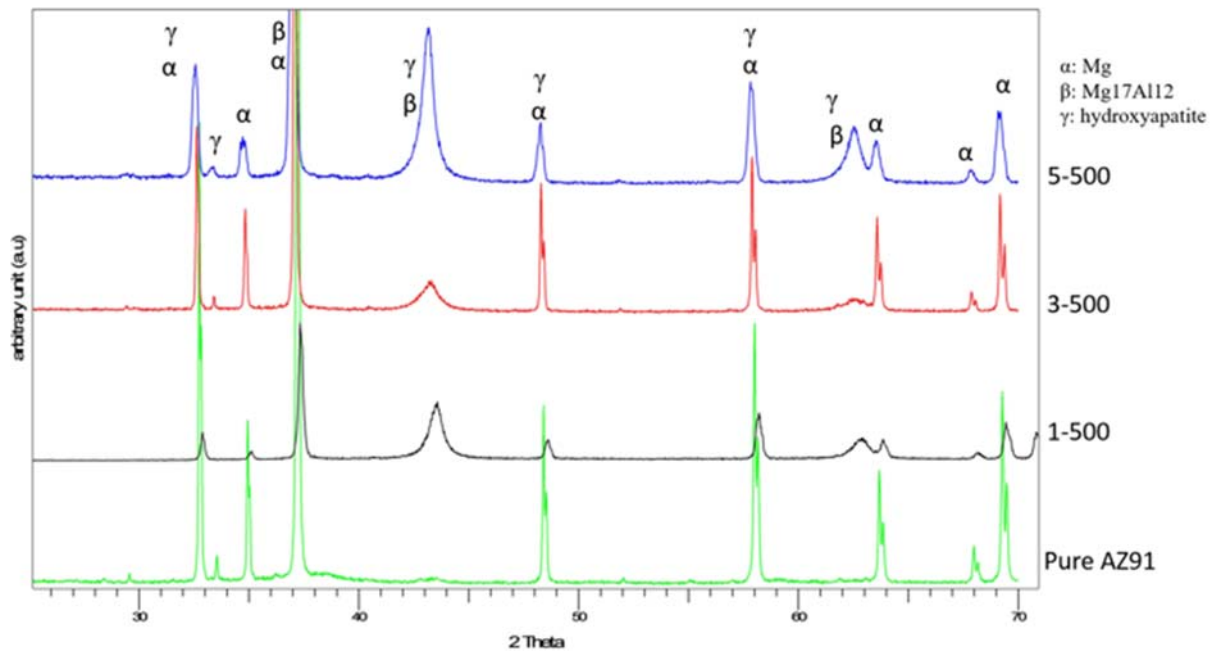


Figure 6. XRD patterns of the coatings sintered at 300, 400, and 500 °C with 1 dip number and pure AZ91 Mg alloy.

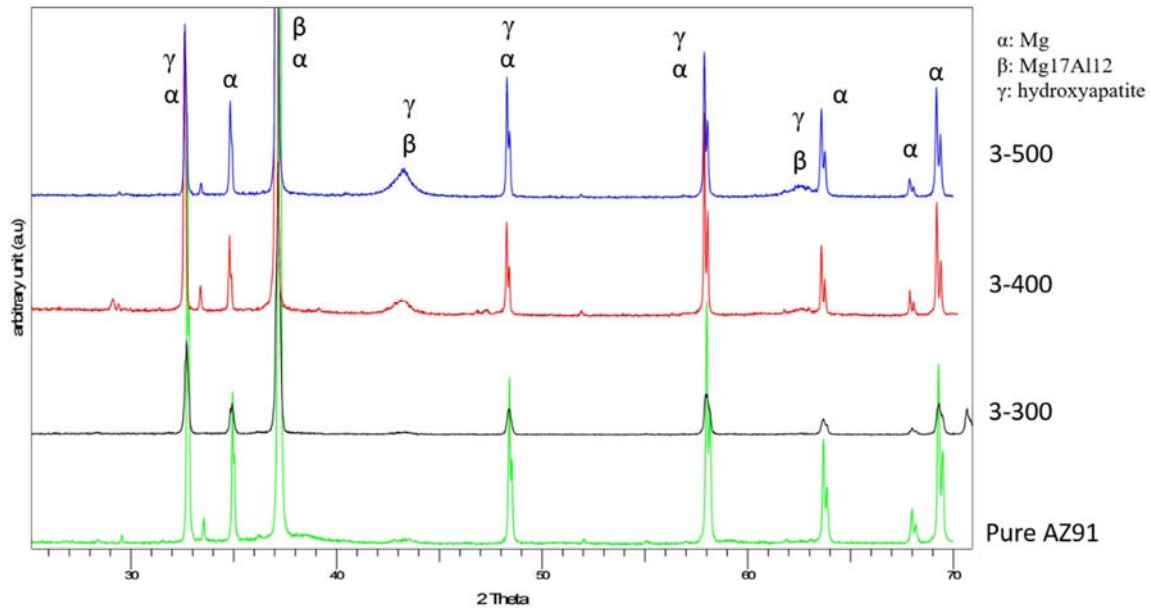


Figure 7. XRD patterns of the coatings sintered at 300, 400, and 500 °C with 3 dip number and pure AZ91 Mg alloy.

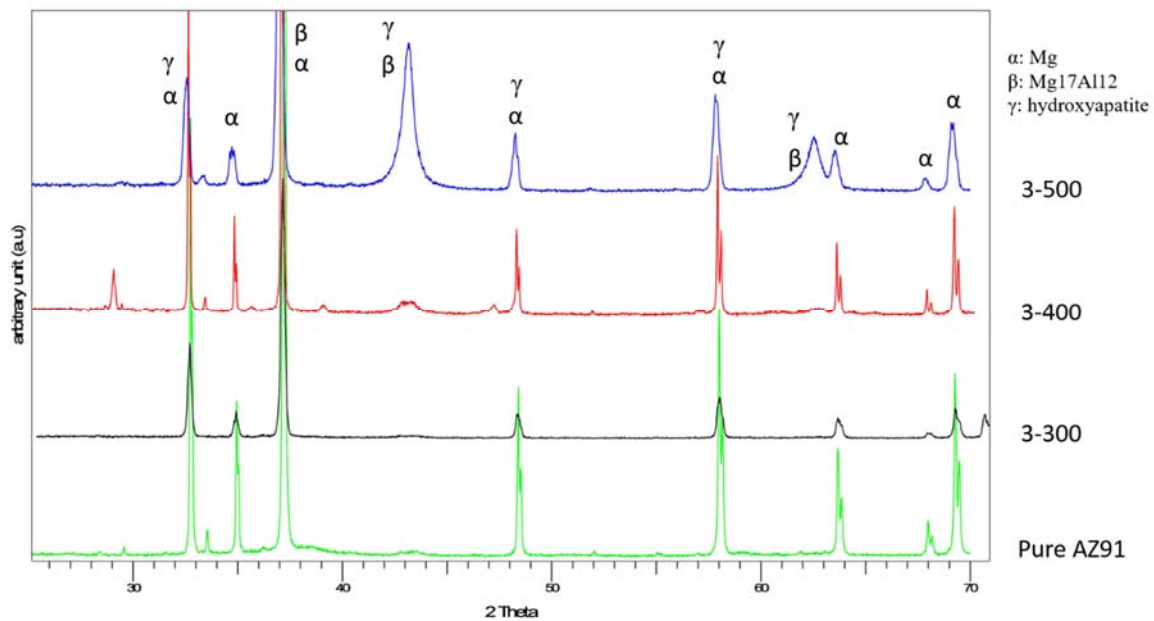


Figure 8. XRD patterns of the coatings sintered at 300, 400, and 500 °C with 5 dip number and pure AZ91 Mg alloy.

Conclusion

AZ91 alloy was produced with hot press sintering method in this study. Produced specimens were coated with hydroxyapatite using combination of sol-gel and dip coating method. The effects of process parameters on coating quality was evaluated with SEM and x-ray diffractometer (XRD). Coating layer thickness is increased with the increasing number of dip. Furthermore, with increasing sintering temperatures, the cracks on the surface of coatings are increased.

References

- Chen, X.-B. , Birbilis, N. , & Abbott, T.B. (2012). Effect of $[Ca^{2+}]$ and $[PO_3^-]$ levels on the formation of calcium phosphate conversion coatings on die-cast magnesium alloy AZ91D. *Corrosion Science*, 55, 226–232.
- Hiromoto, S. , & Yamamotoa, A. (2009). High corrosion resistance of magnesium coated with hydroxyapatite directly synthesized in an aqueous solution. *Electrochimica Acta*, 54, 7085–7093.
- Hiromoto, S., & Tomozawa, M. (2011). Hydroxyapatite coating of AZ31 magnesium alloy by a solution treatment and its corrosion behavior in NaCl solution. *Surface & Coatings Technology*, 205, 4711–4719.
- Hou, D., Liang, S., Chen, R., Dong, C., & Han, E. (2015). Effects of Sb Content on Solidification Pathways and Grain Size of AZ91 Magnesium Alloy. *Acta Metallurgica Sinica*, 28, 115-121 .
- Kabirian, F., & Mahmudi, R. (2009). Impression Creep Behavior of a Cast AZ91 Magnesium Alloy. *Metallurgical and Materials Transactions A*, 40A, 116-127.
- Kannan, M. B. (2015). Electrochemical deposition of calcium phosphates on magnesium and its alloys for improved biodegradation performance: A review. *Surface & Coatings Technology*.
- Lee, D., Pai, Y., & Chang, S. (2013). Effect of Thermal Treatment of the Hydroxyapatite Powders on the Micropore and Microstructure of Porous Biphasic Calcium Phosphate Composite Granules. *Journal of Biomaterials and Nanobiotechnology*, 4, 114-118.
- Liu, G.Y. , Hu, J. , Ding, Z.K. , & Wang, C. . (2011). Formation mechanism of calcium phosphate coating on micro-arc oxidized magnesium. *Materials Chemistry and Physics*, 130, 1118– 1124.
- Liu, G.Y. , Hu, J. , Ding, Z.K., & Wang, C. . (2011). Bioactive calcium phosphate coating formed on micro-arc oxidized magnesium by chemical deposition. *Applied Surface Science*, 257, 2051–2057.
- Niu, B., Shi, P. , Wei, D., E, S., Li, Q., & Chen, Y. (2016). Effects of sintering temperature on the corrosion behavior of AZ31 alloy with Ca-P sol-gel coating. *Journal of Alloys and Compounds*, 665, 435-442.
- Razavi, M., Fathi, M., Savabi, O., Beni, B., Razavi, S., Vashae, D., & Tayebi, L. (2014). Coating of biodegradable magnesium alloy bone implants using nanostructured diopside ($CaMgSi_2O_6$). *Applied Surface Science*, 288, 130– 137.
- Rojaee, R., Fathi, M., & Raeissi, K. (2014). Comparing Nanostructured Hydroxyapatite Coating on AZ91 Alloy Samples via Sol-gel and Electrophoretic Deposition for Biomedical Applications. *IEEE Transactions on NanoBioscience* , 13, 409-414.
- Surmeneva, M.A., & Surmenev, R.A. . (2015). Microstructure characterization and corrosion behaviour of a nanohydroxyapatite coating deposited on AZ31 magnesium alloy using radio frequency magnetron sputtering. *Vacuum*, 117, 60-62.
- Surmeneva, M.A., Tyurinb, A.I., Mukhametkaliyev, T.M., Pirozhkova, T.S., Shuvarin, I.A. , Syrtaov, M.S., & Surmenev, R.A. (2015). Enhancement of the mechanical properties of AZ31 magnesium alloy via nanostructured hydroxyapatite thin films fabricated via radio-frequency magnetron sputtering. *Journal of the mechanical behavior of biomedical materials*, 127–136.
- Wang, M.J., Chao, S.C., & Yen, S.K. (2016). Electrolytic calcium phosphate/zirconia composite coating on AZ91D magnesium alloy for enhancing corrosion resistance and bioactivity . *Corrosion Science*, 47-60.
- Xu, L., Pan, F., Yu, G., Yang, L., Zhang, E., & Yang, K. (2009). In vitro and in vivo evaluation of the surface bioactivity of a calcium phosphate coated magnesium alloy. *Biomaterials*, 30, 1512–1523.